



Mycorrhiza - saprotroph interactions and carbon cycling in the rhizosphere

Journal:	<i>Global Change Biology</i>
Manuscript ID	GCB-24-1752
Wiley - Manuscript type:	Research Article
Date Submitted by the Author:	20-Jun-2024
Complete List of Authors:	Tripathi, Binu; West Virginia University, Department of Biology; West Virginia University, Plant and Soil Sciences Piñeiro Nevado, Juan; Polytechnic University of Madrid, Department of Natural Systems and Resources; West Virginia University, Division of Plant and Soil Sciences Dang, Chansotheary; West Virginia University, Division of Plant and Soil Sciences; Brzostek, Edward; West Virginia University Morrissey, Ember; West Virginia University, Plant and Soil Sciences
Keywords:	Microbial traits, Microbial biomass, Mycorrhiza, Stable isotope probing, Rhizosphere bacteria, Root exudate, Soil carbon, Temperate forest
Abstract:	Labile carbon (C) inputs in soils are expected to increase in the future due to global change drivers such as elevated atmospheric CO ₂ concentrations or warming and potential increases in plant primary productivity. However, the role of mycorrhizal association in modulating microbial activity and soil organic matter (SOM) biogeochemistry responses to increasing below-ground C inputs remains unclear. We employed ¹⁸ O-H ₂ O quantitative stable isotope probing to investigate the effects of synthetic root exudate addition (0, 250, 500, and 1000 µg C g soil ⁻¹) on microbial growth traits and SOM biogeochemistry in rhizosphere soils of trees associated with arbuscular mycorrhizal (AM) and ectomycorrhizal (ECM) fungi. Soil respiration increased proportionally to the amount of exudate addition in both AM and ECM soils. However, microbial biomass C (MBC) responses differed, increasing in AM and decreasing in ECM soils. In AM soils, exudate addition increased taxon-specific and community-wide relative growth rates leading to enhanced production of MBC. Conversely, in ECM soils, relative growth rates were less responsive to exudate addition and estimates of MBC mortality increased with increasing exudate addition. In the AM soils, aggregated microbial growth traits were predictive of soil respiration but this relationship was not observed in ECM soils, perhaps due to substantial MBC mortality. These findings highlight the distinct responses of rhizosphere microbial communities to exudates in AM and ECM-associated trees. Considering that microbial products contribute to the formation of stable soil organic carbon (SOC) pools, future increases in labile exudate release in response to global change may consequently lead to greater SOC gains in AM soils compared ECM soils.



SCHOLARONE™
Manuscripts

1 **Title:** Mycorrhiza - saprotroph interactions and carbon cycling in the rhizosphere

2

3 **Running Title:** Mycorrhiza and saprotroph in rhizosphere

4

5 **List of Authors:** Binu M. Tripathi^{1,2}, Juan Piñeiro^{1,3}, Chansotheary Dang¹, Edward
6 Brzostek², Ember M. Morrissey^{1,2*}

7

8 **Institutional affiliations:**

9 ¹Division of Plant and Soil Sciences, West Virginia University, Morgantown, West Virginia, USA

10 ²Department of Biology, West Virginia University, Morgantown, West Virginia, USA

11 ³School of Forest Engineering and Natural Resources, Polytechnic University of Madrid, Madrid,
12 Spain

13

14 ***Correspondence:**

15 Ember M. Morrissey, Email: ember.morrissey@mail.wvu.edu

16 Abstract

17 Labile carbon (C) inputs in soils are expected to increase in the future due to global change drivers
18 such as elevated atmospheric CO₂ concentrations or warming and potential increases in plant
19 primary productivity. However, the role of mycorrhizal association in modulating microbial
20 activity and soil organic matter (SOM) biogeochemistry responses to increasing below-ground C
21 inputs remains unclear. We employed ¹⁸O–H₂O quantitative stable isotope probing to investigate
22 the effects of synthetic root exudate addition (0, 250, 500, and 1000 µg C g soil⁻¹) on microbial
23 growth traits and SOM biogeochemistry in rhizosphere soils of trees associated with arbuscular
24 mycorrhizal (AM) and ectomycorrhizal (ECM) fungi. Soil respiration increased proportionally to
25 the amount of exudate addition in both AM and ECM soils. However, microbial biomass C (MBC)
26 responses differed, increasing in AM and decreasing in ECM soils. In AM soils, exudate addition
27 increased taxon-specific and community-wide relative growth rates leading to enhanced
28 production of MBC. Conversely, in ECM soils, relative growth rates were less responsive to
29 exudate addition and estimates of MBC mortality increased with increasing exudate addition. In
30 the AM soils, aggregated microbial growth traits were predictive of soil respiration but this
31 relationship was not observed in ECM soils, perhaps due to substantial MBC mortality. These
32 findings highlight the distinct responses of rhizosphere microbial communities to exudates in AM
33 and ECM-associated trees. Considering that microbial products contribute to the formation of
34 stable soil organic carbon (SOC) pools, future increases in labile exudate release in response to
35 global change may consequently lead to greater SOC gains in AM soils compared ECM soils.

36

37 **Keywords:** Microbial traits; Microbial biomass; Mycorrhiza; Stable isotope probing; Rhizosphere
38 bacteria; Root exudate; Soil carbon; Temperate forest

39

40 **1 INTRODUCTION**

41 Interactions between plants, mycorrhiza, and soil microbes in the rhizosphere are a dominant
42 control on the response of soil organic carbon (SOC) and net primary production to global change
43 in temperate forest ecosystems (Terrer et al., 2021). Global change drivers, including elevated
44 CO₂ or warming, often increase the exudation of labile C from fine roots (Phillips et al., 2011; Yin
45 et al., 2013). However, there is uncertainty in the extent to which shifts in rates of root exudation
46 either prime (Cheng et al., 2014) or stabilize soil organic C and nitrogen (N) (Ridgeway et al.,
47 2024). At the center of this uncertainty is a lack of understanding regarding how increases in root
48 exudation in response to global change alter taxon-specific and community-level microbial
49 function.

50 In the temperate forest ecosystem, mycorrhiza colonize the interface between plant roots
51 and soil, effectively regulating the crucial entry point for plant C into the rhizosphere. Arbuscular
52 mycorrhizal (AM) and ectomycorrhizal (ECM) are the two most dominant mycorrhizal types
53 associated with the majority of terrestrial plant species (Brundrett, 2009; Bonfante and Genre,
54 2010). Root exudation rates, and the ability of roots to ramp up exudation rates in response to
55 global change, varies between AM and ECM tree species (Phillips and Fahey, 2006; Phillips et al.,
56 2013; Brzostek et al., 2015). Further, AM and ECM fungi have distinct life strategies with respect
57 to resource acquisition and allocation (Aerts, 2003; Phillips et al., 2013) that alter their interactions
58 with other soil microbes. AM fungi rely on saprotrophs for decomposition and nutrient release
59 (Herman et al., 2012), and as such AM tree species may foster cooperative rhizospheres. Indeed,
60 AM hyphae have been shown to act as conduits for photosynthate C that can feed saprotrophic
61 microbial communities (Kaiser et al., 2015; Paterson et al., 2016; Frey, 2019). In contrast, ECM

62 rhizospheres may foster competitive rhizospheres because ECM fungi possess the capability to
63 produce extracellular enzymes to mine organic N (Martin et al., 2016; Chen et al., 2018) and may
64 suppressing the growth of saprotrophs by enhancing N limitation (Gadgil and Gadgil, 1975;
65 Averill and Hawkes, 2016). These prior studies suggest a dichotomy wherein AM fungi cooperate,
66 while ECM compete, with soil saprotrophs like rhizosphere bacteria. These differing interactions
67 between mycorrhiza and soil saprotrophs (i.e. cooperation vs. competition) may shape microbial
68 function and carbon cycling in rhizosphere soils of AM- and ECM-associated plants as root
69 exudation increases with rising atmospheric CO₂ or warming. Understanding these plant-microbe-
70 soil interactions is crucial for accurately modeling and predicting ecosystem responses to global
71 change (Johnson et al., 2013).

72 Recent advances in quantitative stable isotope probing (qSIP) may enhance our ability to
73 detect cooperative and competitive interactions and connect these microbial activities with carbon
74 cycling process rates in rhizosphere soils. By tracking ¹⁸O labeled water into microbial DNA,
75 taxon-specific growth and biomass production in response to root exudation addition can be
76 quantitatively estimated (Hungate et al., 2015). These taxon-specific traits may then be aggregated
77 for comparison with community-level processes, such as soil respiration rates (Walkup et al. *In*
78 *Review*). Similar approaches have been widely applied in macro-organism ecology, where
79 community-weighted mean (CWM) traits have been used to predict various ecosystem processes
80 (Díaz et al., 2007; Suding et al., 2008; De Bello et al., 2010). However, the application of
81 quantitative trait-based approaches remains limited in microbial ecology (Stone et al., 2021; Wang
82 et al., 2021; Piñeiro et al., 2024), making it unclear how changes in community-level trait
83 measurements correspond to rates of ecosystem processes. As microbes consume and respire
84 carbon during growth, community-level microbial growth and biomass production should

85 correlated with soil respiration rates. However, microbial interactions such as competition, that
86 stimulate microbial turnover, may lead to a disconnect between aggregated microbial growth traits
87 and ecosystem process rates.

88 The aim of this study was to determine how rhizosphere carbon inputs regulate microbial
89 growth, biomass production, and soil carbon cycling in rhizosphere soils associated with AM and
90 ECM tree species. To do this, we sampled rhizosphere soils from canopy-dominant AM and ECM
91 trees in a ~120 year old forested watershed at the Fernow Experimental Forest in West Virginia,
92 USA. To mimic changes in root exudation, we added synthetic root exudates across a range of
93 concentrations (0, 250, 500, and 1000 $\mu\text{g C g soil}^{-1}$) and quantified taxon-specific and community-
94 level bacterial growth and biomass production using ^{18}O qSIP in a lab microcosm study. In AM
95 rhizosphere soils, cooperative interactions between AM fungi and saprotrophs may allow
96 saprotrophs to enhance their growth and biomass production in response to labile C inputs (Frey,
97 2019). However, this might not be the case in ECM systems due to the competitive relationship
98 between ECM fungi and saprotrophs (Averill and Hawkes, 2016). As such we hypothesized that
99 (H_1): increasing labile C inputs will increase microbial growth and biomass production to a greater
100 extent in AM rhizosphere soils than in ECM rhizosphere soil. Furthermore, we hypothesized (H_2)
101 that aggregated microbial growth and biomass production traits would be positively correlated
102 with soil respiration rates. In simpler terms, we expected higher C inputs to stimulate microbial
103 growth, leading to increased soil respiration.

104

105 **2 MATERIALS AND METHODS**

106 *2.1 Site description and soil sampling*

107 For this experiment, we collected soil samples at the Fernow long-term experimental forest
108 (hereafter “Fernow”) (reference watershed 4). The watershed comprises an unmanaged, mature
109 (<100 years old) warm temperate forest stand located in the central Appalachian Mountains in
110 West Virginia, United States (39.03°N, 79.67°W). The dominant tree species include *Acer*
111 *saccharum*, *Liriodendron tulipifera* L., and *Acer rubrum* (AM association, near 40% of the basal
112 area), and *Betula lenta*, *Quercus rubra*, and *Fagus grandifolia* (ECM association, near 30% of the
113 basal area) among other tree species. Soils are coarse-textured Inceptisols of the Berks and Calvin
114 Series (Gilliam et al., 1994).

115 In June 2020 (peak growing season), we sampled five 25 x 25 m plots containing
116 approximately 50% AM and ECM tree species. Mineral soil samples were collected from beneath
117 the canopy of three AM and three ECM trees (dbh >70 cm) within each plot. Around each tree,
118 three soil cores (5 cm diameter, 10 cm depth) were collected and pooled into a composite sample
119 per plot and mycorrhizal type. Rhizosphere soil was collected by gently separating the soil attached
120 to live fine roots following the method outlined by Wollum (1994). Samples were then transported
121 on ice and stored at 4°C in the laboratory. Further, samples were sieved (2 mm), and soil moisture
122 and field capacity were measured. Soil moisture was measured gravimetrically from a soil
123 subsample after drying for 48 h at 100°C. Field capacity was calculated according to Veihmeyer
124 and Hendrickson (1931). We air-dried soil samples for approximately 48 hours, which reduced the
125 gravimetric moisture content from an average of 19.9% to 4.5%. This drying step was necessary
126 to facilitate the addition of ¹⁸O water and exudate solution, achieving optimal soil moisture levels
127 for measuring microbial activities (Morrissey et al., 2017; Foley et al., 2023). Subsamples of dried
128 soil were stored at -80 °C for subsequent molecular analysis (unlabeled t₀ samples).

129

130 *2.2 Laboratory incubations: quantification of C mineralization and MBC*

131 Microcosm incubations were carried out to quantify the amount of CO₂–C respired across different
132 levels of labile C input in AM and ECM rhizosphere soils. The experiment consisted of two soil
133 types (AM and ECM rhizosphere soils) with three synthetic root exudate addition levels (250, 500,
134 and 1000 µg C g soil⁻¹, exudate addition treatment) and a no substrate addition control (water only),
135 each with five replicates (from each plot-level samples), for a total of 40 microcosms. The
136 synthetic root exudate mixture was composed of carbohydrates (23% each of glucose, fructose,
137 and sucrose) and organic acids (11% each of succinic and malic acid, and 9% of aspartic acid). A
138 total of 12 g (dry weight equivalent) soil samples were used to establish microcosms, which were
139 then sealed in 950 mL mason jars, adjusted to 60% water holding capacity with water or exudate
140 solution, and incubated for 5 days in the dark at room temperature (~23 °C). Total CO₂
141 concentration in the headspace of each microcosm was measured on days 1, 3, and 5 using a LI-
142 6400XT (LI-COR Biosciences, Lincoln, NE, USA) similar to Walkup et al. (2020). Following the
143 end of the 5-day incubation, MBC was determined from a subsample of 10 g soil and assessed via
144 the chloroform fumigation extraction method (Witt et al., 2000) followed by persulfate digestion
145 (Doyle et al., 2004) as described in Dang and Morrissey (Dang and Morrissey, 2024). The MBC
146 values were corrected for an extraction efficiency factor of 2.64 (Vance et al., 1987).

147

148 *2.3 Laboratory incubations: quantitative stable isotope probing (qSIP)*

149 A parallel incubation for qSIP used 2 g (dry weight equivalent) of soil per replicate. These samples
150 were placed into 15 ml Falcon tubes and adjusted to 60% water holding capacity (38 ± 5 %
151 gravimetric moisture) with either ¹⁸O water (97 atom %) alone or ¹⁸O water containing synthetic
152 root exudate. The incubation conditions and treatments mirrored those of the C mineralization,

153 except for soil volume and the use of ^{18}O water. The addition of 0.67 ± 0.11 mL of ^{18}O water
154 achieved $75 \pm 15\%$ ^{18}O water enrichment. After the 5-day incubation, soil samples were
155 immediately frozen at -80°C (^{18}O -labelled t_5 samples).

156 Soil DNA was extracted from 0.25 g of each sample using the PowerLyzer PowerSoil DNA
157 Isolation Kit (MoBio Laboratories, Carlsbad, CA, USA) in accordance with the manufacturer's
158 instructions. The DNA was quantified using a Qubit Fluorometer (Life Technologies, Carlsbad,
159 California, USA). Approximately 1.5 μg of DNA from each sample was separated by isopycnic
160 centrifugation using 3.5 ml of saturated CsCl and gradient buffer (200 mM Tris-HCL, 200 mM
161 KCl, 1 mM Ethylenediaminetetraacetic acid at pH 8) solution in a 4.6 ml OptiSeal ultracentrifuge
162 tube (Beckman Coulter, Fullerton, CA). The samples were centrifuged in an Optima Max
163 ultracentrifuge (Beckman Coulter, Indianapolis, IN) using a Beckman TLA 110 rotor at 127,000
164 $\times g$ for 72 h at 18°C . After centrifugation, the density gradient was fractionated by collecting \sim 28-
165 30 fractions (each with 145-155 μl) per sample. The density of each fraction was measured using
166 a Laxco RHD-B Series digital refractometer (Laxco Inc., Mill Creek, WA, USA). The DNA was
167 then precipitated using isopropanol, cleaned with ethanol, and resuspended in 50 μl of nuclease-
168 free water. The 16S rRNA gene abundance of all the fractions was measured using quantitative
169 PCR with primer pair 515F/806R targeting the hypervariable V4 region, as described previously
170 in Walkup et al. (2020). For all samples, fractions within the density range 1.644 to 1.738
171 g mL^{-1} were sequenced for 16S rRNA gene using the Illumina MiSeq sequencing platform
172 (2 \times 250 bp) at the Michigan State University Research Technology Support Facility Genomics
173 Core. All sequence data is available under the NCBI SRA BioProject ID PRJNA1017906.

174

175 *2.4 Data processing and statistical analysis*

176 The resulting 16S rRNA gene sequence data were analyzed using QIIME2 (version.2021.2)
177 (Bolyen et al., 2019). First, the raw forward and reverse sequence reads were imported into the
178 QIIME2 format, and paired-end reads were assembled using the q2-vsearch plugin. To denoise
179 sequences and resolve amplicon sequence variants (ASVs), all reads with low-quality scores or
180 ambiguous base calls were then quality-filtered using the q2-deblur plugin with a trim length of
181 250 bp. The ASVs were taxonomically classified using the q2-feature-classifier (sklearn) trained
182 on the SILVA v138.1 database. The resulting ASV feature table of each qSIP fraction was
183 collapsed at the genus level and imported into R for further analysis. The 16S rRNA gene
184 abundance (qPCR) and sequence read counts from non-fractionated samples were used to calculate
185 the relative abundance of each taxon. The ^{18}O excess atom fraction (EAF) of each taxon was
186 calculated as previously described (Hungate et al., 2015), using a custom R script
187 (<https://bitbucket.org/qsip/>). Briefly, a weighted average density (WAD) was first calculated for
188 each taxon. The difference in WAD (^{18}O -labelled t_5 - unlabeled t_0 samples) was used to quantify
189 the amount of ^{18}O assimilation (^{18}O EAF) by individual taxa. A previously described method
190 (Morrissey et al., 2017) was employed to account for technical error arising from slight variations
191 in CsCl density gradients among ultracentrifuge tubes during WAD calculation. Finally, to
192 determine the labile exudate addition response ($\Delta^{18}\text{O}$ EAF), the ^{18}O EAF values of bacterial taxa
193 in each exudate-amended treatment were subtracted from the values in the no substrate addition
194 control (water only).

195 The relative growth rate (RGR) of each taxon was estimated as a function of the rate of ^{18}O
196 assimilation into DNA, assuming 40% of oxygen atoms derived from ^{18}O -water (based on the
197 maximum observed ^{18}O EAF value of approximately 0.4 in this study). This approach aligns with

198 Purcell et al. (2022) and assumes steady-state microbial populations (Hungate et al., 2015; Li et
199 al., 2019).

200 $RGR_i = EAF_i / (\text{average soil water } {}^{18}\text{O enrichment} \times 0.4)$ (1)

201

202 The microbial community-weighted mean (CWM) of relative growth rate was calculated
203 as follows:

204 $CWM_j = \sum_i^n p_i \times RGR_i$ (2)

205 where p_i is the relative abundance and RGR_i is the relative growth rate of the taxon i in community
206 j , and n is the total number of taxa in the community.

207

208 The production of new microbial biomass ($\mu\text{g C g}^{-1}$ soil) was estimated as the product of
209 the CWM and the community's MBC, as described previously (Wang et al., 2021):

210 $New MBC_j = CWM_j \times MBC_j$ (3)

211

212 To estimate the MBC mortality in each community, we used the following mass balance
213 equation:

214 $(Initial MBC_j + New MBC_j) = (Final MBC_j + MBC_j \text{ Mortality})$ (4)

215 Here, *Initial MBC_j* represents the MBC in community j under water-only treatment (assuming no
216 change in MBC without exudate addition), while *Final MBC_j* refers to the MBC of community j
217 with exudate addition. Rearranging the equation yields:

218 $MBC_j \text{ Mortality} = (Initial MBC_j + New MBC_j) - Final MBC_j$ (5)

219

220 The contribution of each taxon to new biomass production (NB_i) was estimated as the
221 product of its relative abundance (p_i) and its relative growth rate (RGR_i), divided by the sum of the
222 product of relative abundance and growth for all taxa, and then multiplied with new MBC,
223 following Wang et al. (2021).

224
$$NB_i = \frac{p_i \times RGR_i}{\sum_i^n p_i \times RGR_i} \times \text{New MBC} \quad (6)$$

225
226 New MBC production is a crucial factor in understanding both the overall productivity of the
227 microbial community and the growth dynamics of individual taxa within it.

228 All statistical analyses were performed in R version 4.2.1 (Team, 2020). All figures were
229 created using ggplot2. The pairwise Bray-Curtis dissimilarities ('vegdist' function) of
230 compositional profile of microbial communities (non-fractionated DNA samples) were calculated
231 using the "vegan" package (Oksanen et al., 2016) and visualized using principal coordinates
232 analysis (PCoA). Permutational multivariate analysis of variance (PERMANOVA, 'adonis'
233 function, with 999 permutations) was used to assess the effect of labile exudate addition and
234 mycorrhizal type on microbial community composition. Mixed-effects models in "nlme" package
235 (Pinheiro et al., 2017) were employed to test the effects of exudate addition, mycorrhizal
236 association, and their interaction on soil respiration, MBC, CWM, new MBC, and MBC mortality.
237 Sampling plot was included as a random factor to account for variation among plots. Post hoc
238 pairwise comparisons were computed using the 'emmeans' package (Lenth et al., 2019).
239 Correlation analyses between CWM and soil respiration, MBC and soil respiration, and new MBC
240 and soil respiration were conducted in R.

241

242 **3 RESULTS**

243 The PERMANOVA results showed that both exudate addition and mycorrhizal association shaped
244 microbial community composition (Figure S1). However, exudate addition had a stronger impact,
245 explaining roughly 20% of the variation in community structure (PERMANOVA:
246 $R^2 = 0.20, p < 0.001$) compared to mycorrhizal associations (AM and ECM), which explained only
247 about 8% of the variation (PERMANOVA: $R^2 = 0.08, p < 0.01$). Microbial community
248 composition in the highest exudate addition treatment (1000 $\mu\text{g C g soil}^{-1}$) was distinct from the
249 other treatments (Figure S1). This shift in community composition likely resulted from changes in
250 the relative abundance of microbial taxa responsive to exudate addition (Figure S2). Specifically,
251 the relative abundance of *Burkholderia-Caballeronia-Paraburkholderia*, *Dyella*, and *Granulicella*
252 increased while unassigned Xanthobacteraceae, Elsterales, Caulobacteraceae, and *Roseiarcus*
253 decreased sharply in the 1000 μg treatment (Figure S2). While changes in the relative abundance
254 of the aforementioned taxa occurred in both AM and ECM soils, the changes were more
255 pronounced in AM systems. For example, *Burkholderia-Caballeronia-Paraburkholderia*
256 increased 2.2 fold in the AM but only 1.8 fold in the ECM in the 1000 $\mu\text{g C}$ exudate addition
257 treatment. Similarly, 1000 $\mu\text{g C}$ exudate addition treatment decreased *Roseiarcus* relative
258 abundance by 59% in the AM but only 49% in the ECM soils.

259 Soil respiration increased proportionally with the amount of exudate addition in both AM
260 and ECM soils (Figure 1A; Table S1). However, the response of MBC to exudate addition
261 depended on the mycorrhizal association (Figure 1B; Table S1), as evidenced by a significant
262 interaction between exudate addition and mycorrhizal association (Figure 1B; Table S1). Overall,
263 MBC in ECM soils decreased as exudate addition increased, while in AM soils showed the
264 opposite trend (Figure 1B).

265 Exudate addition altered the relative growth rates of individual taxa in both AM and ECM
266 soils, but these effects were generally more pronounced in AM soils (Figure 2). Moreover, the
267 differences in taxon-specific RGRs between AM and ECM soils increased with higher levels of
268 exudate addition. For example, exudate addition tended to increase the RGRs of taxa within
269 Proteobacteria, with these increases being larger in the AM soils (Figure 2). Notably, as the level
270 of exudate addition increased, the differences in RGRs between AM and ECM soils became more
271 pronounced, highlighting the contrasting responses of these ecosystems to exudate availability
272 (Figure 2). Similarly, exudate addition significantly increased the CWM relative growth rates in
273 both soils (Figure 3A; Table S1), with AM soils displaying relatively higher CWM values
274 compared to ECM soils.

275 The production of new MBC increased with exudate addition only in AM soils, remaining
276 relatively constant in the ECM soils (Figure 3B; Table S1). Conversely, estimates of MBC
277 mortality increased with exudate addition in ECM soils (Figure 3C; Table S1), but showed minimal
278 change across all exudate addition levels in AM soils. A few key taxa, including *Dyella*,
279 *Burkholderia-Caballeronia-Paraburkholderia*, and Streptomycetaceae, were responsible for most
280 of the new biomass production within the microbial community (Figure 4). Notably, these
281 taxonomic groups displayed higher new biomass production in the AM soils compared to the ECM
282 soils (Table S2). Interestingly, some taxa that responded positively to exudate addition in the AM
283 soils responded negatively in the ECM soils. For instance, *Dyella* and Streptomycetaceae had
284 reduced new biomass production following exudate addition in the ECM rhizosphere, except for
285 *Dyella* at 1000 µg treatment (Figure 4). Bacterial CWM relative growth rates, MBC, and new
286 MBC production were strongly correlated with soil respiration in the AM soils but not in the ECM

287 soils (Figure 5). Notably, across the exudate addition levels, new microbial biomass production
288 could explain 70% of the variation in soil respiration rates in the AM rhizosphere soil.

289

290 **4 DISCUSSION**

291 As global change continues to alter ecosystem function, understanding how plant-microbe
292 interactions will influence ecosystem responses is of paramount importance. Here, we aimed to
293 determine how mycorrhizal association influences the composition, traits, and carbon processing
294 of rhizosphere bacteria. Plants can respond to global change drivers by modifying the rates of
295 rhizosphere exudation, thereby influencing belowground C-cycling processes and microbial
296 community dynamics (Phillips et al., 2011; Yin et al., 2013). Using a range of exudate additions,
297 we determined that mycorrhizal association influences the ability of rhizosphere bacterial taxa to
298 grow and produce biomass. Specifically, in the rhizosphere of AM trees, microbes were able to
299 enhance their growth in proportion to exudate availability, while in ECM rhizosphere soils, growth
300 and biomass production were comparatively suppressed. These results highlight that the effects of
301 rhizosphere exudation on soil carbon storage depend on the interactions between plants,
302 mycorrhizae, and free-living saprotrophs.

303

304 *4.1 Plant-mycorrhizae-saprotroph interactions following exudate addition*

305 Our findings support the hypothesis (H1) that differences in mycorrhizal association can dictate
306 the responses of rhizosphere microbes to exudate addition. While soil respiration increased
307 proportionally to the amount of exudate addition in both AM and ECM soils (Figure 1A), estimates
308 of MBC exhibited contrasting trends, increasing in AM soils but decreasing in ECM soils (Figure
309 1B). These contrasting responses may reflect fundamentally different microbial dynamics

310 occurring in the rhizospheres of AM and ECM trees. AM fungal hyphae serve as conduits for
311 plant-derived photosynthate C to microbial saprotrophs (Drigo et al., 2010; Kaiser et al., 2015;
312 Frey, 2019), stimulating their growth and activity (Toljander et al., 2007; Chowdhury et al., 2022;
313 Zhang et al., 2022). Our results agree with this past work, as exudate addition led to increases in
314 MBC (Figure 1B), relative growth rates (Figure 2), and new biomass production (Figure 4) in AM
315 soils. Moreover, the aggregated taxon-specific relative growth rates, represented as CWM relative
316 growth rates, increased with exudate addition, particularly in AM soils. This increase in CWM
317 traits in response to exudate addition is a consequence of increases in the relative growth rates of
318 bacterial taxa (Figure 2), many of which increased in relative abundance (Figure S2) following
319 exudate addition. AM fungi can secrete low-molecular-weight organic C exudates (Frey, 2019;
320 Chowdhury et al., 2022; Zhang et al., 2022) that may prime saprotrophs to liberate nutrients in the
321 rhizosphere. Exudates are well known to prime rhizobacteria to enhance soil organic matter
322 decomposition and liberate nutrients (Cheng et al., 2014). However, rhizobacteria can also provide
323 nutrients to their host plants and mycorrhizae via nitrogen fixation and phosphorus solubilization
324 (Zeng et al., 2022). As such, AM fungi may engage in mutualistic interactions with rhizobacteria,
325 delivering exudates in exchange for assistance with nutrient acquisition. Moreover, it has been
326 hypothesized that AM fungal-bacterial relationships may have coevolved (Garbaye, 1994; Olsson
327 et al., 2017), leading to a consistent priming of the bacterial community with labile C exudates
328 secreted through AM fungal hyphae (Paterson et al., 2016; Frey, 2019; Kakouridis et al., 2024).
329 This selection process may have favored members of certain bacterial phyla, such as
330 Proteobacteria and Actinobacteria, which are known to dominate in the AM hyphosphere (Zhang
331 et al., 2022), making them well suited to grow rapidly when exudates are abundant. Our results
332 support this, as many taxa in Proteobacteria and Actinobacteria had larger increases in relative

333 growth rates following exudate addition in the AM rhizosphere than the ECM rhizosphere (Figure
334 2).

335 Conversely, our results suggest ECM fungi limit microbial growth and biomass production
336 when exudates are present. While some taxa increased their relative growth rates in response to
337 exudate addition (Figure 2), these increased growth rates were countered by accelerated microbial
338 biomass mortality (Figure 3C) leading to decreases in new biomass production (Figure 3B and
339 Figure 4). Unlike AM fungi, ECM fungi may rely less on saprotrophs for nutrient acquisition, as
340 they can produce extracellular enzymes to acquire small organic N-containing compounds (Talbot
341 et al., 2008; Tedersoo et al., 2012). This organic N uptake may create nutrient limitation and limit
342 saprotrophic activity, a phenomenon known as the Gadgil effect (Gadgil and Gadgil, 1975).
343 Therefore, N limitation could potentially explain the limited increases in microbial relative growth
344 rates observed at both the individual (Figure 2) and community level (Figure 3A) in ECM soils.
345 Under nutrient-limited conditions, the addition of labile C substrates with a high C:N ratio can
346 cause a decline in the microbial population, potentially due to their inability to adapt to
347 stoichiometric imbalances, thereby promoting microbial turnover (Kaiser et al., 2014). Our results
348 are in agreement with this past work, as we observed substantial MBC mortality following exudate
349 addition in the ECM rhizosphere soils. However, it is possible that other mechanisms, beyond
350 nutrient limitation, could cause the observed responses. ECM fungi can produce a range of
351 secondary metabolites, many of which may have antibiotic properties (Rasanayagam and Jeffries,
352 1992; Olsson et al., 1996). Competition for the added exudates could fuel chemical warfare and
353 other antagonistic interactions in the ECM soils, leading to MBC mortality (Figure 3C) and
354 reducing new biomass production (Figure 4). These antagonistic interactions and the rapid MBC

355 mortality could benefit ECM trees and fungi because MBC mortality could enhance the availability
356 of dissolved organic nitrogen and phosphorus.

357 Our findings demonstrate that AM and ECM-associated rhizospheres exert contrasting
358 influences on bacterial growth and biomass production following exudate addition. Specifically,
359 the AM rhizosphere fostered microbial growth and biomass production following exudate
360 addition, possibly due to positive interactions between AM fungi and bacteria. In contrast,
361 microbial growth was more constrained and mortality was high in the ECM rhizosphere exposed
362 to increasing exudation rates, potentially due to nutrient limitation or antagonistic competition.
363 These results shed light on the intricate responses of microbial communities to labile exudate
364 addition in contrasting soil ecosystems, emphasizing the need for further research to unravel the
365 underlying mechanisms driving these dynamics and their implications for ecosystem functioning.

366

367 *4.2 Taxon-specific responses to exudate addition*

368 The addition of labile exudates in soil selectively favors certain bacterial taxa that exhibit rapid
369 growth in nutrient-rich environments, while many others either grow slowly or remain
370 unresponsive (Fierer et al., 2007; Papp et al., 2020; Stone et al., 2023). Our results support this
371 explanation, as we observed an increase in the relative abundance (Figure S2), growth rate (Figure
372 2), and new biomass production (Figure 4) of some bacterial taxa following exudate addition.
373 Notably, *Dyella* (7.2%) and *Burkholderia-Caballeronia-Paraburkholderia* (8.9%) were among
374 the most abundant genera in both AM and ECM soils. These taxa increased their relative growth
375 rates in response to exudate addition. Both of these genera are well-known rhizobacteria that can
376 produce phytohormones, solubilize phosphate, and fix nitrogen (Palaniappan et al., 2010;
377 Domínguez-Castillo et al., 2021). As such, these bacteria have been reported to colonize the

378 surface of both AM and ECM hyphae (Bonfante and Anca, 2009; Taktek et al., 2015; Marupakula
379 et al., 2017) and likely engage in forming tripartite symbiotic associations with mycorrhizae and
380 their host plants (Zhang et al., 2024). However, the responses of these bacterial taxa to exudate
381 addition were much stronger in AM soils compared to ECM soils. AM fungal hyphae release
382 compounds that enhance SOM priming by stimulating the activity of specific rhizosphere bacteria
383 referred to as ‘hyper symbionts’ (Jansa et al., 2013). *Burkholderia* and *Dyella* are commonly
384 reported from the hyphosphere or mycorrhizosphere of AM fungi (Taktek et al., 2015).
385 Interestingly, despite the positive effect of exudate addition on the relative growth rates of *Dyella*
386 in both AM and ECM rhizospheres, *Dyella* had reduced biomass production in the ECM
387 rhizosphere under certain exudate addition treatments (250 and 500 $\mu\text{g C g soil}^{-1}$), suggesting
388 exudate addition may stimulate rapid turnover in some rhizobacteria populations, where mortality
389 exceeds growth.

390

391 4.3 Connecting microbial growth, biomass production, and ecosystem function

392 The functional trait values within an ecosystem are shaped by the species composition of
393 ecological communities and the prevailing environmental conditions, making trait-based
394 approaches a robust framework for linking organismal responses to environmental changes with
395 shifts in ecosystem functioning (Hicks et al., 2022). The results showed a significant correlation
396 between CWM relative growth rates and soil respiration with exudate addition in AM soils (Figure
397 5A). Moreover, there was an even stronger relationship between newly synthesized MBC and soil
398 respiration in AM soils (Figure 5C). The new MBC represents the proportion of microbial biomass
399 synthesized over the course of the experimental incubation and approximates the growth of
400 metabolically active bacteria, therefore offering better predictability for soil processes. The

401 connection between CWM relative growth rate and new biomass production suggests soil
402 respiration in AM soil was driven by the need for energy production to fuel growth in response to
403 exudate addition. Further, our findings agree with past qSIP-based studies that identified CWM
404 traits (Piñeiro et al., 2024, Walkup et al. In Review) and new biomass production (Wang et al.
405 2021) as predictive of soil respiration. For instance, reductions in the C and N assimilation traits
406 of bacterial communities under chronic N deposition mirrored decreases in soil respiration and N
407 mineralization in AM forest soils (Piñeiro et al., 2024). Our approach to calculating CWM relative
408 growth rates focused only on bacteria, and thus may have been more successful in the AM
409 rhizosphere where bacteria are posited to play a larger role. Relative to ECM systems, AM
410 ecosystems are characterized by a higher bacteria to fungi ratio (Cheeke et al., 2017) and a greater
411 proportion of bacterial genes linked to nutrient and C cycling (Bahram et al., 2020), highlighting
412 the importance of bacterial saprotrophs in AM soil function (Carrara et al., 2021; Piñeiro et al.,
413 2024). Linking microbial community composition to function is a long-standing challenge in
414 microbial ecology, and our results suggest that the trait-based framework provides an appropriate
415 measure to connect microbial diversity with ecosystem functions (Morrissey et al., 2023).

416 In contrast, none of the community-level microbial traits (CWM, MBC, and new MBC)
417 showed a significant correlation with soil respiration in ECM soils, indicating a decoupling
418 between community-level traits and soil processes in these environments, as previously reported
419 (Piñeiro et al., 2024). This disconnect highlights that other microbial dynamics or populations may
420 be needed to accurately understand soil respiration in the ECM rhizosphere. Perhaps most notably,
421 our results suggest that high MBC turnover (Figure 3C) may have fueled CO₂ production in the
422 ECM rhizosphere. This turnover could be driven by nutrient limitation or antibiosis as described
423 above. For instance, the ECM rhizosphere could be particularly deficient in N due to N mining by

424 ECM fungi (Phillips et al., 2013). To overcome N deficiency, microorganisms in these soils would
425 likely switch to necromass-N recycling to cope with acute stoichiometric imbalances under high
426 C input (Kaiser et al., 2014; Cui et al., 2020), resulting in C overflow as increased microbial
427 respiration (Manzoni et al., 2008; Spohn, 2015). In this scenario, microbes relying on labile C
428 would increase their growth rate (Reischke et al., 2014; Wei et al., 2019), but with minimal changes
429 in their biomass likely due to their shortened lifespan (Behera and Wagner, 1974), facilitating
430 necromass generation and rapid microbial turnover. Such dynamics could explain how exudate
431 addition increased soil respiration (Figure 1) but resulted in limited increases in taxon-specific and
432 CWM relative growth rates (Figure 2, Figure 3a) and no increases in biomass production (Figure
433 3B). Alternatively, the disconnect could relate to the absence of fungal communities in our
434 calculation of community-level traits. Given the dominance of fungi in ECM soils (Cheeke et al.,
435 2017), their inclusion may be necessary to establish connections between microbial traits and soil
436 processes (Averill et al., 2014; Carrara et al., 2021).

437 Taken together our results suggest that AM ecosystems will respond very differently from
438 ECM ecosystems to increases in root exudation, likely associated with global change drivers such
439 as elevated atmospheric CO₂ or warming. Increased root exudation in AM ecosystems would
440 stimulate microbial growth in the rhizosphere, leading to greater biomass production. As this
441 microbial biomass gradually turns over, the resulting microbial residues could contribute to the
442 formation of mineral-associated organic matter (MAOM) (Sokol et al., 2019), thereby increasing
443 the SOC stock in AM ecosystems (Keller et al., 2021). MAOM cycles slowly and shields C from
444 microbial decomposition (Schlesinger and Lichter, 2001), making it a significant process for
445 enhancing the long-term carbon sequestration potential of AM ecosystems. In contrast, the
446 enhanced exudation in ECM ecosystems may not fuel microbial growth and biomass production

447 as significantly due to increased microbial mortality and rapid microbial necromass recycling. This
448 dynamic could result in smaller changes in the stable SOC pool in ECM ecosystems under global
449 change drivers such as elevated CO₂ levels and warming.

450

451 **5 CONCLUSIONS**

452 In summary, labile exudates elicited contrasting responses in rhizosphere bacteria between AM
453 and ECM ecosystems. Taxon-specific relative growth rates and new biomass production increased
454 more in AM soils after exudate addition. Similarly, CWM traits, reflecting aggregated taxon-
455 specific relative growth rates, further increased in AM soils. These findings suggest that while new
456 biomass production thrived in AM soils with exudate addition, it declined in ECM soils, potentially
457 due to accelerated microbial mortality. Notably, community-level aggregated traits predicted soil
458 respiration, MBC, and new MBC in AM soils, but not in ECM soils. This discrepancy might be
459 linked to mycorrhizal-driven interactions with saprotrophic bacteria within these contrasting
460 ecosystems. The strong correlation between bacterial community composition traits and soil
461 processes in the AM system underscores the crucial role of bacterial saprotrophs in AM soil
462 functioning. Overall, our results demonstrate that the trait-based framework offers a valuable tool
463 to connect microbial diversity with ecosystem functions, and plant-mycorrhizae-saprotroph
464 interactions determine the fate of root exudation and shape ecosystem feedbacks to global change.

465

466 **ACKNOWLEDGEMENTS**

467 This work was supported by the U.S. Department of Energy award DE-SC0019472 and the
468 National Science Foundation, Division of Environmental Biology Award 2114570. Juan Piñeiro

469 was supported by the Ramón y Cajal program from the Spanish Ministry of Sciences (RYC-2021-
470 033454)

471

472 **CONFLICT OF INTEREST STATEMENT**

473 The authors declare no conflicts of interest.

474

475 **DATA AVAILABILITY STATEMENT**

476 The sequence data and related metadata are accessible under the NCBI
477 SRA BioProject ID PRJNA1017906.

478

479 **REFERENCES**

480 Aerts, R. (2003) The role of various types of mycorrhizal fungi in nutrient cycling and plant
481 competition. In *Mycorrhizal Ecology*: Springer, pp. 117-133.

482 Averill, C., and Hawkes, C.V. (2016) Ectomycorrhizal fungi slow soil carbon cycling. *Ecology*
483 *Letters* **19**: 937-947.

484 Averill, C., Turner, B.L., and Finzi, A.C. (2014) Mycorrhiza-mediated competition between
485 plants and decomposers drives soil carbon storage. *Nature* **505**: 543-545.

486 Bahram, M., Netherway, T., Hildebrand, F., Pritsch, K., Drenkhan, R., Loit, K. et al. (2020)
487 Plant nutrient-acquisition strategies drive topsoil microbiome structure and function. *New*
488 *Phytologist* **227**: 1189-1199.

489 Behera, B., and Wagner, G. (1974) Microbial growth rate in glucose-amended soil. *Soil Science*
490 *Society of America Journal* **38**: 591-594.

491 Bolyen, E., Rideout, J., Dillon, M., Bokulich, N., Abnet, C., Al-Ghalith, G. et al. (2019)
492 Reproducible, interactive, scalable and extensible microbiome data science using QIIME
493 2. *Nature Biotechnology* **37**: 852-857.

494 Bonfante, P., and Anca, I.-A. (2009) Plants, mycorrhizal fungi, and bacteria: a network of
495 interactions. *Annual Review of Microbiology* **63**: 363-383.

496 Bonfante, P., and Genre, A. (2010) Mechanisms underlying beneficial plant–fungus interactions
497 in mycorrhizal symbiosis. *Nature Communications* **1**: 48.

498 Brundrett, M.C. (2009) Mycorrhizal associations and other means of nutrition of vascular plants:
499 understanding the global diversity of host plants by resolving conflicting information and
500 developing reliable means of diagnosis. *Plant and Soil* **320**: 37-77.

501 Brzostek, E.R., Dragoni, D., Brown, Z.A., and Phillips, R.P. (2015) Mycorrhizal type determines
502 the magnitude and direction of root-induced changes in decomposition in a temperate
503 forest. *New Phytologist* **206**: 1274-1282.

504 Carrara, J.E., Walter, C.A., Freedman, Z.B., Hostetler, A.N., Hawkins, J.S., Fernandez, I.J., and
505 Brzostek, E.R. (2021) Differences in microbial community response to nitrogen
506 fertilization result in unique enzyme shifts between arbuscular and
507 ectomycorrhizal-dominated soils. *Global Change Biology* **27**: 2049-2060.

508 Cheeke, T.E., Phillips, R.P., Brzostek, E.R., Rosling, A., Bever, J.D., and Fransson, P. (2017)
509 Dominant mycorrhizal association of trees alters carbon and nutrient cycling by selecting
510 for microbial groups with distinct enzyme function. *New Phytologist* **214**: 432-442.

511 Chen, W., Koide, R.T., and Eissenstat, D.M. (2018) Nutrient foraging by mycorrhizas: from
512 species functional traits to ecosystem processes. *Functional Ecology* **32**: 858-869.

513 Cheng, W., Parton, W.J., Gonzalez-Meler, M.A., Phillips, R., Asao, S., McNickle, G.G. et al.

514 (2014) Synthesis and modeling perspectives of rhizosphere priming. *New Phytologist*

515 **201**: 31-44.

516 Chowdhury, S., Lange, M., Malik, A.A., Goodall, T., Huang, J., Griffiths, R.I., and Gleixner, G.

517 (2022) Plants with arbuscular mycorrhizal fungi efficiently acquire Nitrogen from

518 substrate additions by shaping the decomposer community composition and their net

519 plant carbon demand. *Plant and Soil* **475**: 473-490.

520 Cui, J., Zhu, Z., Xu, X., Liu, S., Jones, D.L., Kuzyakov, Y. et al. (2020) Carbon and nitrogen

521 recycling from microbial necromass to cope with C: N stoichiometric imbalance by

522 priming. *Soil Biology and Biochemistry* **142**: 107720.

523 Dang, C., and Morrissey, E.M. (2024) The size and diversity of microbes determine carbon use

524 efficiency in soil. *Environmental Microbiology* **26**: e16633.

525 De Bello, F., Lavorel, S., Díaz, S., Harrington, R., Cornelissen, J.H., Bardgett, R.D. et al. (2010)

526 Towards an assessment of multiple ecosystem processes and services via functional traits.

527 *Biodiversity and Conservation* **19**: 2873-2893.

528 Domínguez-Castillo, C., Alatorre-Cruz, J.M., Castañeda-Antonio, D., Munive, J.A., Guo, X.,

529 López-Olguín, J.F. et al. (2021) Potential seed germination-enhancing plant growth-

530 promoting rhizobacteria for restoration of *Pinus chiapensis* ecosystems. *Journal of*

531 *Forestry Research* **32**: 2143-2153.

532 Doyle, A., Weintraub, M.N., and Schimel, J.P. (2004) Persulfate digestion and simultaneous

533 colorimetric analysis of carbon and nitrogen in soil extracts. *Soil Science Society of*

534 *America Journal* **68**: 669-676.

535 Drigo, B., Pijl, A.S., Duyts, H., Kielak, A.M., Gamper, H.A., Houtekamer, M.J. et al. (2010)
536 Shifting carbon flow from roots into associated microbial communities in response to
537 elevated atmospheric CO₂. *Proceedings of the National Academy of Sciences* **107**: 10938-
538 10942.

539 Díaz, S., Lavorel, S., De Bello, F., Quétier, F., Grigulis, K., and Robson, T.M. (2007)
540 Incorporating plant functional diversity effects in ecosystem service assessments.
541 *Proceedings of the National Academy of Sciences* **104**: 20684-20689.

542 Fierer, N., Bradford, M.A., and Jackson, R.B. (2007) Toward an ecological classification of soil
543 bacteria. *Ecology* **88**: 1354-1364.

544 Foley, M.M., Blazewicz, S.J., McFarlane, K.J., Greenlon, A., Hayer, M., Kimbrel, J.A. et al.
545 (2023) Active populations and growth of soil microorganisms are framed by mean annual
546 precipitation in three California annual grasslands. *Soil Biology and Biochemistry* **177**:
547 108886.

548 Frey, S.D. (2019) Mycorrhizal fungi as mediators of soil organic matter dynamics. *Annual
549 Review of Ecology, Evolution, and Systematics* **50**: 237-259.

550 Gadgil, P.D., and Gadgil, R.L. (1975) Suppression of litter decomposition by mycorrhizal roots
551 of *Pinus radiata*. *New Zealand Journal of Forestry Science* **5**: 33-41.

552 Garbaye, J. (1994) Tansley review no. 76 helper bacteria: a new dimension to the mycorrhizal
553 symbiosis. *New Phytologist* **128**: 197-210.

554 Gilliam, F.S., Turrill, N.L., Aulick, S.D., Evans, D.K., and Adams, M.B. (1994) Herbaceous
555 layer and soil response to experimental acidification in a central Appalachian hardwood
556 forest. *Journal of Environmental Quality* **23**: 835-844.

557 Hendrickson, A., and Veihmeyer, F. (1931) Influence of dry soil on root extension. *Plant*
558 *Physiology* **6**: 567.

559 Herman, D.J., Firestone, M.K., Nuccio, E., and Hodge, A. (2012) Interactions between an
560 arbuscular mycorrhizal fungus and a soil microbial community mediating litter
561 decomposition. *FEMS Microbiology Ecology* **80**: 236-247.

562 Hicks, L.C., Frey, B., Kjøller, R., Lukac, M., Moora, M., Weedon, J.T., and Rousk, J. (2022)
563 Toward a function-first framework to make soil microbial ecology predictive. *Ecology*
564 **103**: e03594.

565 Hungate, B., Mau, R., Schwartz, E., Caporaso, J., Dijkstra, P., van Gestel, N. et al. (2015)
566 Quantitative Microbial Ecology through Stable Isotope Probing. *Applied and*
567 *Environmental Microbiology* **81**: 7570-7581.

568 Jansa, J., Bukovská, P., and Gryndler, M. (2013) Mycorrhizal hyphae as ecological niche for
569 highly specialized hypersymbionts—or just soil free-riders? *Frontiers in Plant Science* **4**:
570 50022.

571 Johnson, N.C., Angelard, C., Sanders, I.R., and Kiers, E.T. (2013) Predicting community and
572 ecosystem outcomes of mycorrhizal responses to global change. *Ecology Letters* **16**: 140-
573 153.

574 Kaiser, C., Franklin, O., Dieckmann, U., and Richter, A. (2014) Microbial community dynamics
575 alleviate stoichiometric constraints during litter decay. *Ecology Letters* **17**: 680-690.

576 Kaiser, C., Kilburn, M.R., Clode, P.L., Fuchslueger, L., Koranda, M., Cliff, J.B. et al. (2015)
577 Exploring the transfer of recent plant photosynthates to soil microbes: mycorrhizal
578 pathway vs direct root exudation. *New Phytologist* **205**: 1537-1551.

579 Kakouridis, A., Yuan, M., Nuccio, E.E., Hagen, J.A., Fossum, C.A., Moore, M.L. et al. (2024)
580 Arbuscular mycorrhiza convey significant plant carbon to a diverse hyphosphere
581 microbial food web and mineral-associated organic matter. *New Phytologist* **242**: 1661-
582 1675.

583 Keller, A.B., Brzostek, E.R., Craig, M.E., Fisher, J.B., and Phillips, R.P. (2021) Root-derived
584 inputs are major contributors to soil carbon in temperate forests, but vary by mycorrhizal
585 type. *Ecology Letters* **24**: 626-635.

586 Lenth, R., Singmann, H., Love, J., Buerkner, P., and Herve, M. (2019) Emmeans: Estimated
587 marginal means, aka least-squares means. R package version 1.7.2-9000003.

588 Li, J., Mau, R., Dijkstra, P., Koch, B., Schwartz, E., Liu, X. et al. (2019) Predictive genomic
589 traits for bacterial growth in culture versus actual growth in soil. *The ISME Journal* **13**:
590 2162-2172.

591 Manzoni, S., Jackson, R.B., Trofymow, J.A., and Porporato, A. (2008) The global stoichiometry
592 of litter nitrogen mineralization. *Science* **321**: 684-686.

593 Martin, F., Kohler, A., Murat, C., Veneault-Fourrey, C., and Hibbett, D.S. (2016) Unearthing the
594 roots of ectomycorrhizal symbioses. *Nature Reviews Microbiology* **14**: 760-773.

595 Marupakula, S., Mahmood, S., Jernberg, J., Nallanchakravarthula, S., Fahad, Z.A., and Finlay,
596 R.D. (2017) Bacterial microbiomes of individual ectomycorrhizal *Pinus sylvestris* roots
597 are shaped by soil horizon and differentially sensitive to nitrogen addition. *Environmental*
598 *Microbiology* **19**: 4736-4753.

599 Morrissey, E.M., Mau, R.L., Schwartz, E., McHugh, T.A., Dijkstra, P., Koch, B.J. et al. (2017)
600 Bacterial carbon use plasticity, phylogenetic diversity and the priming of soil organic
601 matter. *The ISME Journal* **11**: 1890-1899.

602 Morrissey, E.M., Kane, J., Tripathi, B.M., Rion, M.S.I., Hungate, B.A., Franklin, R. et al. (2023)
603 Carbon acquisition ecological strategies to connect soil microbial biodiversity and carbon
604 cycling. *Soil Biology and Biochemistry* **177**: 108893.

605 Oksanen, J., Blanchet, F., Kindt, R., Legendre, P., Minchin, P., O'Hara, R. et al. (2016) Vegan:
606 community ecology package. R Package version 2.4-1.

607 Olsson, P.A., Chalot, M., Bååth, E., Finlay, R.D., and Söderström, B. (1996) Ectomycorrhizal
608 mycelia reduce bacterial activity in a sandy soil. *FEMS Microbiology Ecology* **21**: 77-86.

609 Olsson, S., Bonfante, P., and Pawłowska, T.E. (2017) Ecology and evolution of fungal-bacterial
610 interactions. In *The Fungal Community Its Organization and Role in the Ecosystem,*
611 *Fourth Edition*: CRC Press Taylor & Francis Group, pp. 563-584.

612 Palaniappan, P., Chauhan, P.S., Saravanan, V.S., Anandham, R., and Sa, T. (2010) Isolation and
613 characterization of plant growth promoting endophytic bacterial isolates from root nodule
614 of Lespedeza sp. *Biology and Fertility of Soils* **46**: 807-816.

615 Papp, K., Hungate, B.A., and Schwartz, E. (2020) Glucose triggers strong taxon-specific
616 responses in microbial growth and activity: insights from DNA and RNA qSIP. *Ecology*
617 **101**: e02887.

618 Paterson, E., Sim, A., Davidson, J., and Daniell, T.J. (2016) Arbuscular mycorrhizal hyphae
619 promote priming of native soil organic matter mineralisation. *Plant and Soil* **408**: 243-
620 254.

621 Phillips, R.P., and Fahey, T.J. (2006) Tree species and mycorrhizal associations influence the
622 magnitude of rhizosphere effects. *Ecology* **87**: 1302-1313.

623 Phillips, R.P., Finzi, A.C., and Bernhardt, E.S. (2011) Enhanced root exudation induces
624 microbial feedbacks to N cycling in a pine forest under long-term CO₂ fumigation.
625 *Ecology Letters* **14**: 187-194.

626 Phillips, R.P., Brzostek, E., and Midgley, M.G. (2013) The mycorrhizal-associated nutrient
627 economy: a new framework for predicting carbon–nutrient couplings in temperate
628 forests. *New Phytologist* **199**: 41-51.

629 Pinheiro, J., Bates, D., DebRoy, S., Sarkar, D., Heisterkamp, S., Van Willigen, B., and
630 Maintainer, R. (2017) Package ‘nlme’. *Linear and nonlinear mixed effects models*,
631 *version 3*: 274.

632 Piñeiro, J., Dang, C., Walkup, J.G., Kuzniar, T., Winslett, R., Blazewicz, S.J. et al. (2024) Shifts
633 in bacterial traits under chronic nitrogen deposition align with soil processes in
634 arbuscular, but not ectomycorrhizal-associated trees. *Global Change Biology* **30**: e17030.

635 Purcell, A.M., Hayer, M., Koch, B.J., Mau, R.L., Blazewicz, S.J., Dijkstra, P. et al. (2022)
636 Decreased growth of wild soil microbes after 15 years of transplant-induced warming in a
637 montane meadow. *Global Change Biology* **28**: 128-139.

638 Rasanayagam, S., and Jeffries, P. (1992) Production of acid is responsible for antibiosis by some
639 ectomycorrhizal fungi. *Mycological Research* **96**: 971-976.

640 Reischke, S., Rousk, J., and Bååth, E. (2014) The effects of glucose loading rates on bacterial
641 and fungal growth in soil. *Soil Biology and Biochemistry* **70**: 88-95.

642 Ridgeway, J., Kane, J., Morrissey, E., Starcher, H., and Brzostek, E. (2024) Roots selectively
643 decompose litter to mine nitrogen and build new soil carbon. *Ecology Letters* **27**: e14331.

644 Schlesinger, W.H., and Lichter, J. (2001) Limited carbon storage in soil and litter of
645 experimental forest plots under increased atmospheric CO₂. *Nature* **411**: 466-469.

646 Sokol, N.W., Sanderman, J., and Bradford, M.A. (2019) Pathways of mineral-associated soil
647 organic matter formation: Integrating the role of plant carbon source, chemistry, and
648 point of entry. *Global Change Biology* **25**: 12-24.

649 Spohn, M. (2015) Microbial respiration per unit microbial biomass depends on litter layer
650 carbon-to-nitrogen ratio. *Biogeosciences* **12**: 817-823.

651 Stone, B.W., Li, J., Koch, B.J., Blazewicz, S.J., Dijkstra, P., Hayer, M. et al. (2021) Nutrients
652 cause consolidation of soil carbon flux to small proportion of bacterial community.
653 *Nature Communications* **12**: 3381.

654 Stone, B.W., Dijkstra, P., Finley, B.K., Fitzpatrick, R., Foley, M.M., Hayer, M. et al. (2023) Life
655 history strategies among soil bacteria—dichotomy for few, continuum for many. *The
656 ISME Journal* **17**: 611-619.

657 Suding, K.N., Lavorel, S., Chapin III, F., Cornelissen, J.H., Diaz, S., Garnier, E. et al. (2008)
658 Scaling environmental change through the community-level: A trait-based
659 response-and-effect framework for plants. *Global Change Biology* **14**: 1125-1140.

660 Taktek, S., Trépanier, M., Servin, P.M., St-Arnaud, M., Piché, Y., Fortin, J.-A., and Antoun, H.
661 (2015) Trapping of phosphate solubilizing bacteria on hyphae of the arbuscular
662 mycorrhizal fungus Rhizophagus irregularis DAOM 197198. *Soil Biology and
663 Biochemistry* **90**: 1-9.

664 Talbot, J., Allison, S., and Treseder, K. (2008) Decomposers in disguise: mycorrhizal fungi as
665 regulators of soil C dynamics in ecosystems under global change. *Functional Ecology* **22**:
666 955-963.

667 Team, R.C. (2020) R Core Team R: a language and environment for statistical computing.
668 *Foundation for Statistical Computing*.

669 Tedersoo, L., Bahram, M., Toots, M., Diedhiou, A.G., Henkel, T.W., Kjøller, R. et al. (2012)
670 Towards global patterns in the diversity and community structure of ectomycorrhizal
671 fungi. *Molecular Ecology* **21**: 4160-4170.

672 Terrer, C., Phillips, R.P., Hungate, B.A., Rosende, J., Pett-Ridge, J., Craig, M.E. et al. (2021) A
673 trade-off between plant and soil carbon storage under elevated CO₂. *Nature* **591**: 599-
674 603.

675 Toljander, J.F., Lindahl, B.D., Paul, L.R., Elfstrand, M., and Finlay, R.D. (2007) Influence of
676 arbuscular mycorrhizal mycelial exudates on soil bacterial growth and community
677 structure. *FEMS Microbiology Ecology* **61**: 295-304.

678 Vance, E.D., Brookes, P.C., and Jenkinson, D.S. (1987) An extraction method for measuring soil
679 microbial biomass C. *Soil Biology and Biochemistry* **19**: 703-707.

680 Walkup, J., Freedman, Z., Kotcon, J., and Morrissey, E. (2020) Pasture in crop rotations
681 influences microbial biodiversity and function reducing the potential for nitrogen loss
682 from compost. *Agriculture Ecosystems and Environment* **304**.

683 Wang, C., Morrissey, E., Mau, R., Hayer, M., Pineiro, J., Mack, M. et al. (2021) The temperature
684 sensitivity of soil: microbial biodiversity, growth, and carbon mineralization. *The ISME
685 Journal* **15**: 2738-2747.

686 Wei, X., Zhu, Z., Wei, L., Wu, J., and Ge, T. (2019) Biogeochemical cycles of key elements in
687 the paddy-rice rhizosphere: microbial mechanisms and coupling processes. *Rhizosphere*
688 **10**: 100145.

689 Witt, C., Gaunt, J.L., Galicia, C.C., Ottow, J.C., and Neue, H.-U. (2000) A rapid chloroform-
690 fumigation extraction method for measuring soil microbial biomass carbon and nitrogen
691 in flooded rice soils. *Biology and Fertility of Soils* **30**: 510-519.

692 Wollum, A. (1994) Soil sampling for microbiological analysis. *Methods of Soil Analysis: Part 2*

693 *Microbiological and Biochemical Properties* **5**: 1-14.

694 Yin, H., Li, Y., Xiao, J., Xu, Z., Cheng, X., and Liu, Q. (2013) Enhanced root exudation

695 stimulates soil nitrogen transformations in a subalpine coniferous forest under

696 experimental warming. *Global Change Biology* **19**: 2158-2167.

697 Zeng, Q., Ding, X., Wang, J., Han, X., Iqbal, H.M., and Bilal, M. (2022) Insight into soil

698 nitrogen and phosphorus availability and agricultural sustainability by plant growth-

699 promoting rhizobacteria. *Environmental Science and Pollution Research* **29**: 45089-

700 45106.

701 Zhang, C., van der Heijden, M.G., Dodds, B.K., Nguyen, T.B., Spooren, J., Valzano-Held, A. et

702 al. (2024) A tripartite bacterial-fungal-plant symbiosis in the mycorrhiza-shaped

703 microbiome drives plant growth and mycorrhization. *Microbiome* **12**: 13.

704 Zhang, L., Zhou, J., George, T.S., Limpens, E., and Feng, G. (2022) Arbuscular mycorrhizal

705 fungi conducting the hyphosphere bacterial orchestra. *Trends in Plant Science*.

706

707 **FIGURE LEGENDS**

708 **FIGURE 1** Soil respiration rate (**A**) and microbial biomass carbon (**B**) in AM and ECM soils with
709 different levels of C input (250 - 1000 $\mu\text{g C g soil}^{-1}$). Significant p values are denoted by asterisks
710 ($***p < 0.001$).

711

712 **FIGURE 2** The change in relative growth rate ($\Delta^{18}\text{O RGR}$) following exudate addition for select
713 microbial taxa (which showed $\Delta^{18}\text{O RGR} > 0.1$ in any of the treatments) that responded to exudate
714 addition (250, 500, and 1000 $\mu\text{g C g soil}^{-1}$) in AM and ECM rhizosphere soils. Different colors
715 indicate the phylum-level microbial taxonomy.

716

717 **FIGURE 3** Community weighted mean (CWM) relative growth rates (A), new MBC production
718 (B), and MBC mortality (C) in AM and ECM soils along the C input gradient. The asterisks
719 indicate p values of the test statistic ($*p < 0.05$; $**p < 0.01$; $***p < 0.001$).

720

721 **FIGURE 4** Change in new biomass (ΔNB_i) between exudate amended soils (250, 500, and 1000
722 $\mu\text{g C g soil}^{-1}$) and unamended soils for selected microbial taxa that demonstrated changes in their
723 biomass production in both AM and ECM rhizosphere soils. Data are mean \pm SE and colored by
724 phylum, note square root scale.

725

726 **FIGURE 5** Relationship between soil respiration rate and CWM relative growth rates, MBC, and
727 new MBC production in AM (A, B, and C) and ECM (D, E, and F) soils along the exudate addition
728 gradient. Significant p -values are represented by asterisks ($***p < 0.001$).

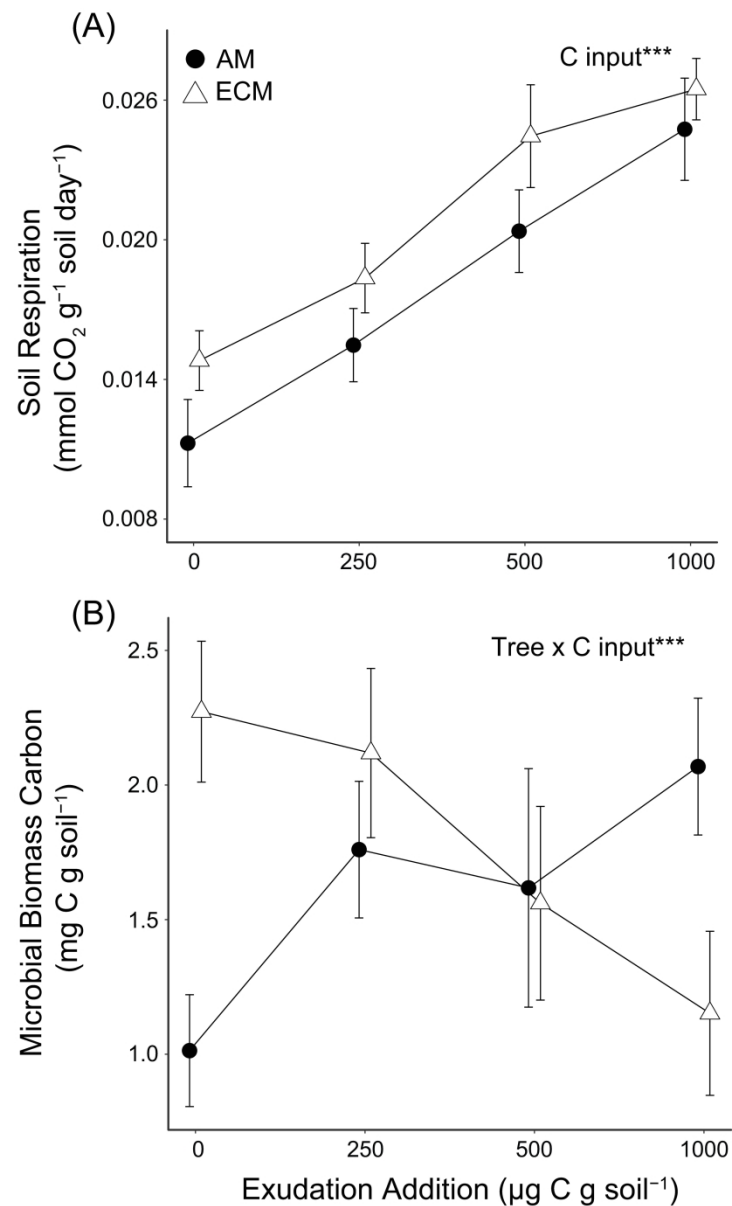


FIGURE 1 Soil respiration rate (A) and microbial biomass carbon (B) in AM and ECM soils with different levels of C input (250 - 1000 $\mu\text{g C g soil}^{-1}$). Significant p values are denoted by asterisks (**p < 0.001).

272x453mm (300 x 300 DPI)

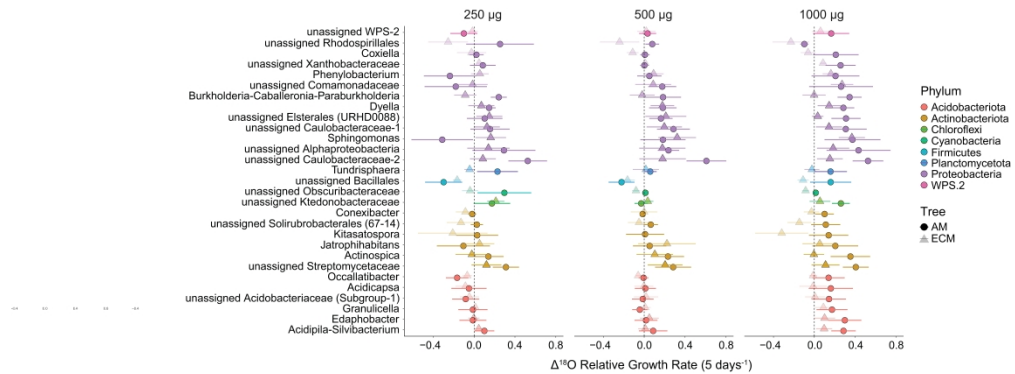


FIGURE 2 The change in relative growth rate ($\Delta^{18}\text{O}$ RGR) following exudate addition for select microbial taxa (which showed $\Delta^{18}\text{O}$ RGR > 0.1 in any of the treatments) that responded to exudate addition (250, 500, and 1000 μg C g soil^{-1}) in AM and ECM rhizosphere soils. Different colors indicate the phylum-level microbial taxonomy.

913x332mm (600 x 600 DPI)

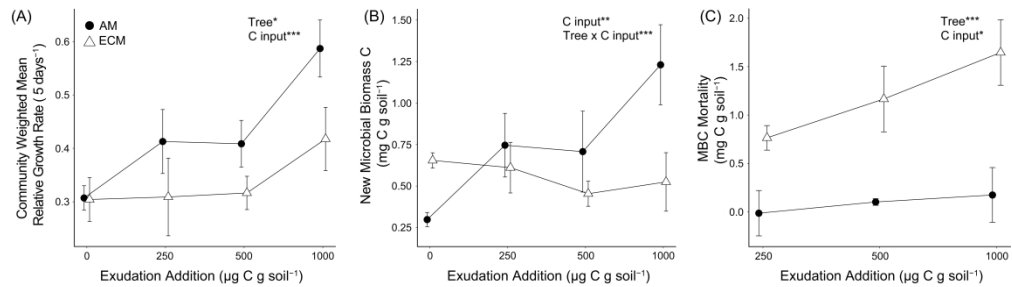


FIGURE 3 Community weighted mean (CWM) relative growth rates (A), new MBC production (B), and MBC mortality (C) in AM and ECM soils along the C input gradient. The asterisks indicate p values of the test statistic (* $p < 0.05$; ** $p < 0.01$; *** $p < 0.001$).

817x225mm (300 x 300 DPI)

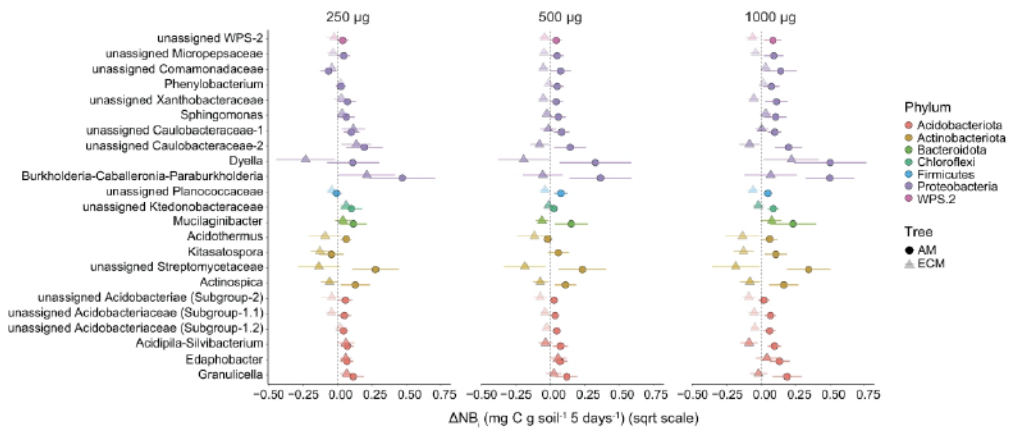


FIGURE 4 Change in new biomass (ΔNB_i) between exudate amended soils (250, 500, and 1000 $\mu\text{g C g soil}^{-1}$) and unamended soils for selected microbial taxa that demonstrated changes in their biomass production in both AM and ECM rhizosphere soils. Data are mean \pm SE and colored by phylum, note square root scale.

795x337mm (600 x 600 DPI)

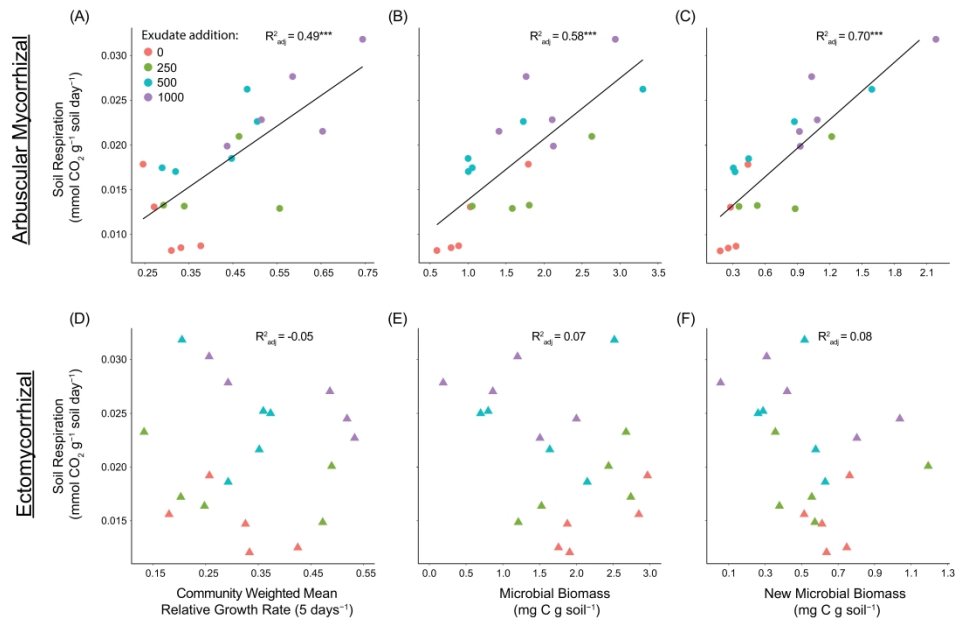


FIGURE 5 Relationship between soil respiration rate and CWM relative growth rates, MBC, and new MBC production in AM (A, B, and C) and ECM (D, E, and F) soils along the exudate addition gradient. Significant p-values are represented by asterisks (**p < 0.001).

824x503mm (600 x 600 DPI)